

AD-A195 073

TRANSVERSE EXPANSION OF INDIVIDUAL CARBON AND GRAPHITE
FILAMENTS... (U) AEROSPACE CORP EL SEGUNDO CA MATERIALS
SCIENCES LAB P M SHEPHERD 22 APR 88

1/1

UNCLASSIFIED

TR-8886A(2935-06)-2 SD-TR-88-51

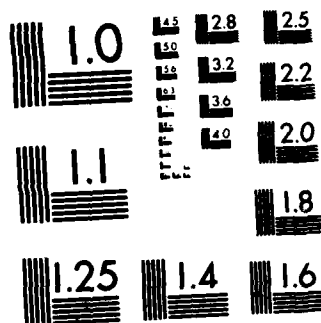
F/G 11/2.1

NL

END
DATE
FILMED
8 8

Table I. The Transverse Coefficient of Thermal Expansion

Average CTE of
Each Filament



MICROCOPY RESOLUTION TEST CHART
NATIONAL BUREAU OF STANDARDS 1963 A

AD-A195 073

APPROVED FOR PUBLIC RELEASE;
DISTRIBUTION UNLIMITED

88 5 16 071

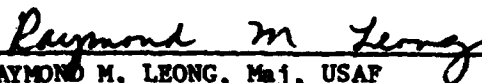
This report was submitted by The Aerospace Corporation, El Segundo, CA 90245, under Contract No. F04701-85-C-0086 with the Space Division, P.O. Box 92960, Worldway Postal Center, Los Angeles, CA 90009-2960. It was reviewed and approved for The Aerospace Corporation by R. W. Fillers, Director, Materials Sciences Laboratory. Capt Donald Thoma, SD/CLVT, was the project officer for the Mission-Oriented Investigation and Experimentation (MOIE) program.

This report has been reviewed by the Public Affairs Office (PAS) and is releasable to the National Technical Information Service (NTIS). At NTIS, it will be available to the general public, including foreign nationals.

This technical report has been reviewed and is approved for publication. Publication of this report does not constitute Air Force approval of the report's findings or conclusions. It is published only for the exchange and stimulation of ideas.



DONALD THOMA, Capt, USAF
MOIE Project Officer
SD/CLVT



RAYMOND M. LEONG, Maj, USAF
Deputy Director, AFSTC West Coast Office
AFSTC/WCO OL-AB

UNCLASSIFIED

SECURITY CLASSIFICATION OF THIS PAGE

REPORT DOCUMENTATION PAGE				
1a. REPORT SECURITY CLASSIFICATION Unclassified			1b. RESTRICTIVE MARKINGS	
2a. SECURITY CLASSIFICATION AUTHORITY			3. DISTRIBUTION / AVAILABILITY OF REPORT Approved for public release; distribution unlimited.	
2b. DECLASSIFICATION / DOWNGRADING SCHEDULE				
4. PERFORMING ORGANIZATION REPORT NUMBER(S) TR-0086A(2935-06)-2			5. MONITORING ORGANIZATION REPORT NUMBER(S) SD-TR-88-51	
6a. NAME OF PERFORMING ORGANIZATION The Aerospace Corporation Laboratory Operations		6b. OFFICE SYMBOL (If applicable)	7a. NAME OF MONITORING ORGANIZATION Space Division	
6c. ADDRESS (City, State, and ZIP Code) El Segundo, CA 90245			7b. ADDRESS (City, State, and ZIP Code) Los Angeles Air Force Base Los Angeles, CA 90009-2960	
8a. NAME OF FUNDING / SPONSORING ORGANIZATION		8b. OFFICE SYMBOL (If applicable)	9. PROCUREMENT INSTRUMENT IDENTIFICATION NUMBER FO4701-85-C-0086	
8c. ADDRESS (City, State, and ZIP Code)			10. SOURCE OF FUNDING NUMBERS	
			PROGRAM ELEMENT NO. PROJECT NO. TASK NO. WORK UNIT ACCESSION NO.	
11. TITLE (Include Security Classification) Transverse Expansion of Individual Carbon and Graphite Filaments				
12. PERSONAL AUTHOR(S) Sheaffer, Patrick M.				
13a. TYPE OF REPORT		13b. TIME COVERED FROM TO	14. DATE OF REPORT (Year, Month, Day) 1988 April 22	15. PAGE COUNT 20
16. SUPPLEMENTARY NOTATION				
17. COSATI CODES			18. SUBJECT TERMS (Continue on reverse if necessary and identify by block number)	
FIELD	GROUP	SUB-GROUP	Thermal expansion, Carbon	
			Thermal strain, Composites	
			Carbon filaments, Graphite	
19. ABSTRACT (Continue on reverse if necessary and identify by block number) The laser diffraction technique for measuring the diameter of fine filaments has been adapted for measuring the transverse coefficient of thermal expansion (CTE) of individual carbon and graphite filaments. CTE was measured on three types of polyacrylonitrile (PAN)-derived filaments and one type of pitch-derived filament that had already been heat-treated to 2600°C. The measurements are unique because the filaments were in a surface-traction-free environment; the data are therefore inherently more accurate than those obtained by conventional methods. Significant variations in the transverse CTE of pitch-based filaments were observed; they have been attributed to local differences in the (transverse) preferred orientation of the graphitic layer planes in those filaments. Individual pitch-based filaments were found to twist about their axis when constrained at both ends and heated; the center of the filament presumably undergoes maximum deflection. <i>Kay</i>				
20. DISTRIBUTION / AVAILABILITY OF ABSTRACT <input type="checkbox"/> UNCLASSIFIED/UNLIMITED <input checked="" type="checkbox"/> SAME AS RPT. <input type="checkbox"/> DTIC USERS			21. ABSTRACT SECURITY CLASSIFICATION Unclassified	
22a. NAME OF RESPONSIBLE INDIVIDUAL			22b. TELEPHONE (Include Area Code)	22c. OFFICE SYMBOL

DD FORM 1473, 84 MAR

83 APR edition may be used until exhausted.
All other editions are obsolete.

SECURITY CLASSIFICATION OF THIS PAGE

UNCLASSIFIED

PREFACE

The author kindly thanks Mr. Barry Sinsheimer and Dr. Leslie Feldman for valuable discussions without which this work would have been much more difficult to complete. Thanks also to Dr. Jack White and Mr. J. Stephen Evangelides for freely lending the benefit of their scientific research experience. I am grateful to Mr. James Noblet and Mr. Herbert Hoppe for providing key solutions to certain problems and to Ms. Laana Fishman, Mr. Curtis Fincher, and their associates for their kind help in providing experimental facilities. This report was prepared with the gracious help and forbearance of Ms. Marian Branch.



Accession For	
NTIS CRA&I	<input checked="checked" type="checkbox"/>
DTIC TAB	<input type="checkbox"/>
Unannounced	<input type="checkbox"/>
Justification	
By	
Date	
Availability Codes	
Dist	Avail and for Special
A-1	

CONTENTS

PREFACE.....	1
I. INTRODUCTION.....	7
II. EXPERIMENTAL.....	9
III. RESULTS.....	15
IV. CONCLUSIONS.....	23
REFERENCES.....	25

FIGURES

1.	Photomicrographs of P55, G50, and AS-1 filaments after heat treatment to 2600°C.....	11
2.	Diagram of test setup and detail of sample holder.....	12
3.	Thermal expansion $\Delta d/d_0$ versus temperature for G50 filaments.....	16
4.	Thermal expansion $\Delta d/d_0$ versus temperature for P55 filaments.....	17
5.	Thermal expansion $\Delta d/d_0$ versus temperature for tungsten filaments.....	18
6.	Apparatus for observing heating-induced twisting in carbon filaments.....	19

TABLE

I.	The Transverse Coefficient of Thermal Expansion.....	13
----	--	----

I. INTRODUCTION

Progress in composite modeling has been hindered by a lack of knowledge about certain constituent material properties, knowledge that would provide a better understanding of the relationship between the composite's structure and its bulk properties. One important property of any composite is its dimensional change in response to variations in temperature. When the constituent materials of a composite vary widely in their thermal strain behavior, the bulk thermal strain behavior of the finished composite is difficult or impossible to predict accurately. There are theoretical treatments of the problem in the literature that are variously successful at approaching an accurate solution.¹ However, all such treatments are limited by the accuracy of the available data on the mechanical and thermal strain behaviors of the composite's constituent materials,² as well as by the simplifying assumptions made in the theory.¹ Mechanical and thermal strain data can be obtained relatively easily for the matrix materials, which can be examined in bulk, but the very small size of the filamentary reinforcement materials poses significant problems for measurement.

Carbon filaments have emerged as important reinforcement materials and are combined with many types of matrices. Because such filaments are small (typically 10 μm in diameter) and highly anisotropic, certain of their properties have been difficult to measure directly. The value of one of these properties--the transverse (diametral) coefficient of thermal expansion (CTE)--is usually determined by incorporating the filaments in a composite with a well-behaved matrix and measuring the composite's bulk thermal expansion. The transverse thermal expansion data for the composite is then used to mathematically "back out" the transverse thermal expansion of the filaments. This technique has been faulted, however, because its accuracy relies on how well the algorithm for modeling the composite fits the microstress environment present in the composite. For example, although there is generally a large amount of debonding between the filament reinforcement and the matrix in carbon-carbon composites, debonding is generally neglected in the models for

generating expansion algorithms.¹ It is therefore desirable to measure the transverse CTE of these filaments in a surface-traction-free environment, i.e., as individual, bare filaments, to provide data that can be applied universally to many types of composites.

The laser diffraction technique³ of filament diameter measurement has been adapted in this work to measure the transverse thermal expansion of individual carbon filaments. This technique employs the Fraunhofer (slit) approximation, $d = L\lambda/D$, where d is the filament diameter, λ is the wavelength of the laser light, L is the distance from the filament to the measurement plane, and D is the distance between adjacent minima in the diffraction pattern. When a carbon filament is placed with its axis perpendicular to, and in the path of, a beam of laser light, it diffracts the light similarly to a lath or slit of width equal to the filament diameter. One can then measure the diffraction pattern and use the Fraunhofer formula to calculate the diameter of the filament. The filament is then heated and again measured to obtain data with which to calculate the transverse thermal expansion.

The Fraunhofer approximation's error for filaments has been evaluated in Ref. 3 as about -3% of the actual filament diameter. This error can be treated as a constant if the filament diameter does not change more than a few percent upon heating (which it does not) and if the index of refraction of the filament remains constant. For this work, the filament index of refraction was assumed not to change appreciably over the temperature range; the optical extinction coefficient of the filament does not vary significantly over the temperature range; and a small change in the filament's reflectivity is not considered important.*

*Data presented by P. Gagnaire, et al. at the 18th Biennial Conference on Carbon indicate that the error is indeed constant for all values of the index of refraction typical of graphite if the laser light is polarized in the TM mode, as it was in this work.

II. EXPERIMENTAL

Four types of carbon filaments were examined in this experiment:

Name	Manufacturer	Precursor
HM 3000	Hercules	PAN
AS-1	Hercules	PAN
G50	Celanese	PAN
P55 (VSB-32T)	Union Carbide ^a	Pitch

^aNow Amoco.

With the exception of VSB-32T (P55), filaments were selected for study on the bases of their circular cross section and lack of surface wrinkles (crenulations), to minimize errors that would be induced if the filaments twisted during heating. Before the filaments were removed from the sample yarns, they were heat-treated in a graphite tube furnace to 2600°C under argon for 10 min to stabilize them against permanent dimensional change and to ensure that any thermally induced twisting of the filaments during the thermal expansion measurements would be recoverable and, therefore, detectable. Recoverable means that any heat-induced twist in the filaments during a CTE measurement will "unwind" upon cool-down and the sample will return to a state of zero twist.

At elevated temperatures, sample twisting is manifested as a random diameter change whose magnitude relates more to the eccentricity of the filament cross section than to the temperature at which the measurements are made. If the twist in the sample filament is small, the overall effect of the apparent strains would be to increase the noise level of the data because the apparent strain can be either positive or negative in sign. Thus, if the filaments twist during the test, the twist will be manifested in an increase in data scatter in the elevated-temperature data, but not in the room-temperature data. Others have noted the tendency of carbon filaments to twist

with heating.⁴ Photomicrographs of the filaments in cross section are shown in Fig. 1.

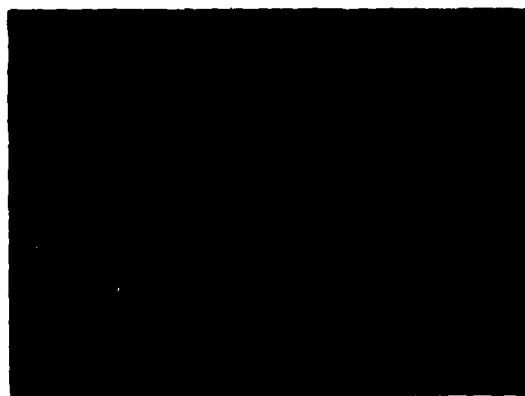
The experimental setup, diagrammed in Fig. 2, consists of a laser source; a sample chamber that can be evacuated to prevent atmospheric interactions; and a medium for recording the diffraction pattern generated by the filament, in this case, type 1-N glass spectrographic film plates. The laser source was a Liconix 401 He-Cd laser ($\lambda = 4416 \text{ \AA}$). The components were mounted on an optical bench for stability. The laser beam was focused to a $40\text{-}\mu\text{m}$ spot over the filament to restrict the length of filament examined in each test. The sample mounts consisted of two end supports of fine copper wire that were flattened and to which a filament could be cemented with conductive colloidal silver. The sample was heated to incandescence by a current that was passed through it. The sample temperature was measured with a Pyrometer Instruments Co. MicroOptical pyrometer. Changes in sample temperature as small as 15°C could be observed, but the overall error was estimated to be $\pm 25^\circ\text{C}$. The measured sample temperatures were corrected for emissivity variations.⁵ Because optical pyrometry was used, measurements were limited to room temperature and temperatures between 600 and 1600°C .

In a typical run, the sample chamber was evacuated overnight to a pressure of $\sim 5 \times 10^{-4}$ Torr. The laser was then switched on, and a card was placed at the film plane to examine the diffraction pattern and adjust the laser beam precisely over the filament. Data were taken by heating the sample, measuring the temperature, adjusting the filament position, and exposing the filament to the laser. The current was then switched off. Sample cooling was virtually instantaneous. This process was performed for each elevated-temperature data point and could be carried out in about 45 sec. Room-temperature data points were taken between each elevated-temperature data point.

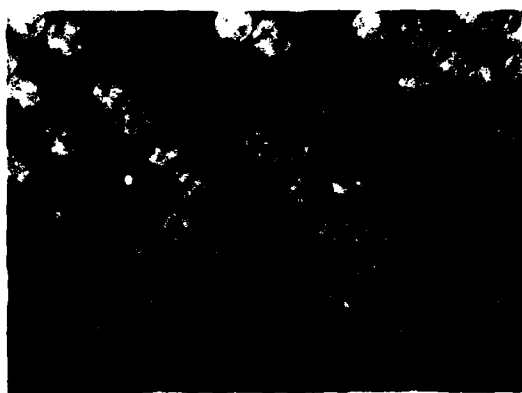
Initially it was speculated that sublimation or oxidation of the filaments would result from short exposures to high temperature; however, no evidence of diameter decrease as a function of time at high temperature was noted in the carbon filaments. One sample of tungsten (Table 1) manifested



(a)



(b)



(c)

Figure 1. Photomicrographs of (a) P55, (b) G50, and (c) AS-1 filaments after heat treatment to 2600°C. Partially crossed polarizers. The optical textures caused by the birefringent graphitic layer planes in the sample microstructures indicate that the PAN filaments are rotationally isotropic (axisymmetric) whereas the P55 filaments are not.

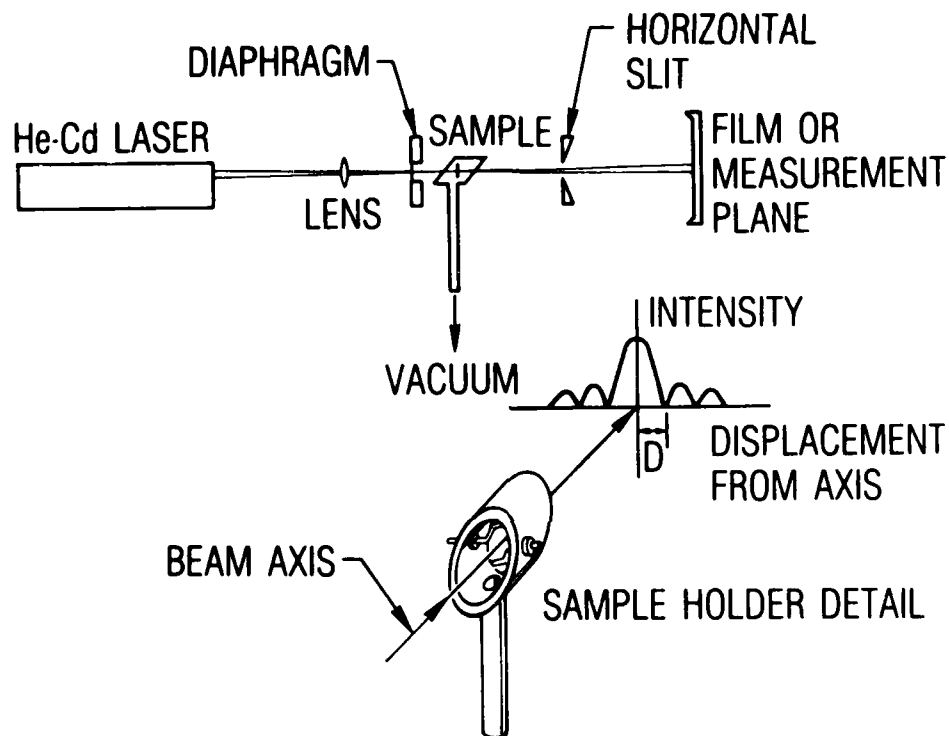


Figure 2. Diagram of test setup and detail of sample holder. The ends of the sample holder are cut to hold windows that form Brewster's angle with the incoming laser beam. The sample chamber was evacuated to prevent oxidation of the sample or refraction of the diffracted light by hot inert gases near the sample surface.

Table 1. The Transverse Coefficient of Thermal Expansion

Sample Diameter d_0 (μm)	s.d. ^a	CTE ($10^{-6} \text{ }^\circ\text{C}^{-1}$)	Correlation Coefficient	Average CTE of Each Filament Type ($10^{-6} \text{ }^\circ\text{C}^{-1}$)	
				\bar{x}	s.d. ^b
HM-3000 (Hercules)					
7.669	0.015	12.6	0.968	10.9	0.83
7.206	0.010	12.1	0.981		
7.628	0.012	9.4	0.918		
7.427	0.010	9.6	0.971		
G50 (Celanese)					
6.371	0.020	13.7	0.948	13.1	0.66
6.483	0.008	11.2	0.987		
6.073	0.008	14.2	0.987		
4.059	0.011	13.3	0.968		
P55 (VSB-32T; Union Carbide)					
11.3	0.018	16.6	0.978	12.0	2.9
9.626	0.021	12.9	0.941		
11.425	0.016	6.6	0.862		
AS-1 (Hercules)					
7.239	0.030	14.3	0.951	12.5	1.2
6.957	0.010	12.9	0.983		
7.091	0.006	10.3	0.974		
Tungsten					
21.633	0.021	5.4	0.929	5.3	0.4
26.135	c	5.8	0.920		
25.775	c	5.8	0.833		
26.176	0.036	4.1	0.626		

^aThe standard deviation of 6 to 8 room-temperature diameter readings per sample.

^bStandard deviation of the mean ($= \sigma/\sqrt{N}$).

^cThese samples were oxidizing during test, so the room-temperature diameter was not constant.

such a decrease, but whether it was due to sublimation of either the tungsten metal or its oxide was unclear. For that sample, the thermal expansion data were analyzed by taking the room-temperature data point immediately following a given elevated-temperature data point and calculating $\Delta d/d_0$ with just the two values. The individual $\Delta d/d_0$ points for each temperature were then combined to calculate the CTE. Because the sample was cooled rapidly after the elevated-temperature data point was taken, negligible diameter change occurred in the interim; therefore, the data are accurate (see Table I). For the other samples, d_0 was determined by averaging all the d_0 data points. Table I indicates that the room-temperature d_0 measurements are very reproducible.

Five to seven elevated-temperature data points and five to 10 room-temperature data points were taken for each sample filament. The film plates were scanned on a Jarrell-Ash scanning microdensitometer to magnify and convert the data to x-y format (film transmittance versus distance from optical axis). The minima were located by drawing intersecting lines on the adjacent slopes of a minimum in the x-y plot, and the point of intersection of those lines was taken as the location of the minimum. Tungsten filaments were measured to assess overall accuracy of the technique. The values for the CTE of the tungsten filaments measured in this work agree satisfactorily with the published National Bureau of Standards data for tungsten (Table I).

III. RESULTS

Figures 3 and 4 are the plotted data for the G50 and P55 filaments, respectively. For comparison, Fig. 5 shows data for the tungsten filaments.

The plots of all three PAN filament types are similar. The P55 filaments are unique in their large elevated-temperature data spread, which is attributed to the thermally induced twisting of the sample filaments. Although the data spread at elevated temperature was much larger for the P55 filaments than for the PAN filaments, the standard deviations in Table I indicate that the room-temperature data spread for all the filaments was similar, consistent with the assumption that the filaments untwist upon cool-down, returning to their equilibrium position.

To investigate the twisting behavior of these filaments, we conducted an experiment in which a P55 filament was slowly twisted while being held taut (to prevent loop formation). The result was that the filament could withstand at least 100π rad of twist per centimeter of length without breaking. In another experiment, a test filament was mounted the same as for the expansion experiments, except that another 1-cm length of filament was bonded at the midpoint of the test filament, transversely to its axis, with colloidal carbon (Fig. 6). When the test filament was heated, the end of the transverse filament was observed to move as the test filament twisted in response to the temperature increase. The end of the transverse filament moved about $1/30$ th of its distance from the test filament axis, a distance corresponding to a twist of $\sim 1.9 \times 10^{-3} \text{ deg cm}^{-1} \text{ }^{\circ}\text{C}^{-1}$. This small amount of twist is of the correct order of magnitude to produce the scatter seen in the P55 elevated-temperature data. Given the eccentricity of the P55 filament cross sections (~ 0.15), a twist as large as 90 deg would result in an apparent $\Delta d/d_0$ of $\sim 1 \times 10^{-1}$ --two orders of magnitude larger than the scatter actually observed.

In addition to the twist-induced scatter in their elevated-temperature data, P55 filaments also exhibit transverse expansivities that vary from filament to filament (see Fig. 4). The photomicrographs in Fig. 1 help to

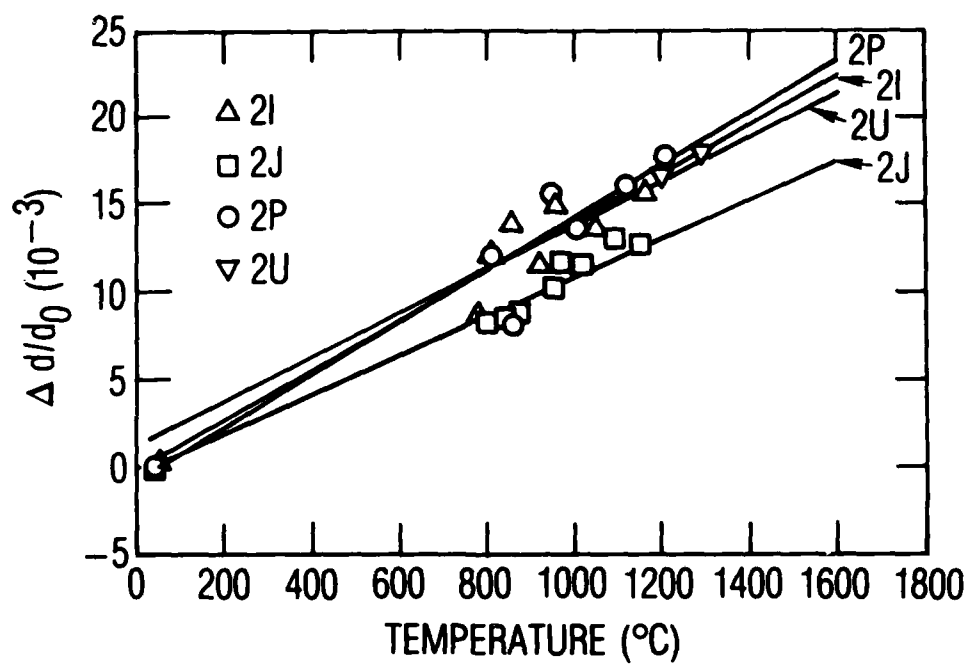


Figure 3. Thermal expansion $\Delta d/d_0$ versus temperature for G50 filaments. Individual sample data are indicated. Lines were derived by linear regression through indicated data and a point at room temperature defined as $\Delta d/d_0 = 0$.

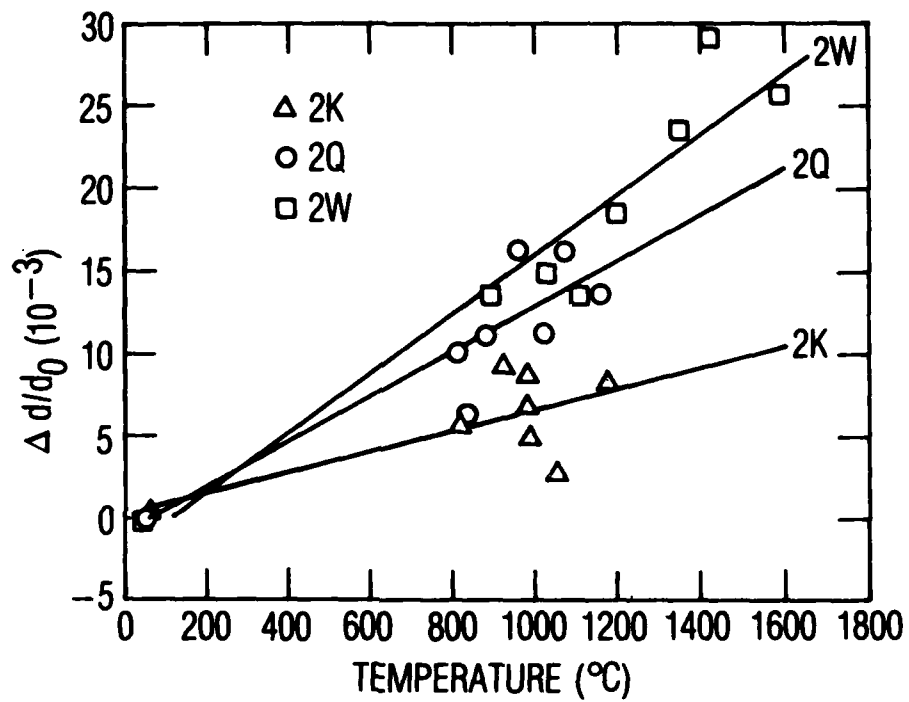


Figure 4. Thermal expansion $\Delta d/d_0$ versus temperature for P55 filaments. Individual sample data are indicated. Lines were derived by linear regression through indicated data and a point at room temperature defined as $\Delta d/d_0 = 0$.

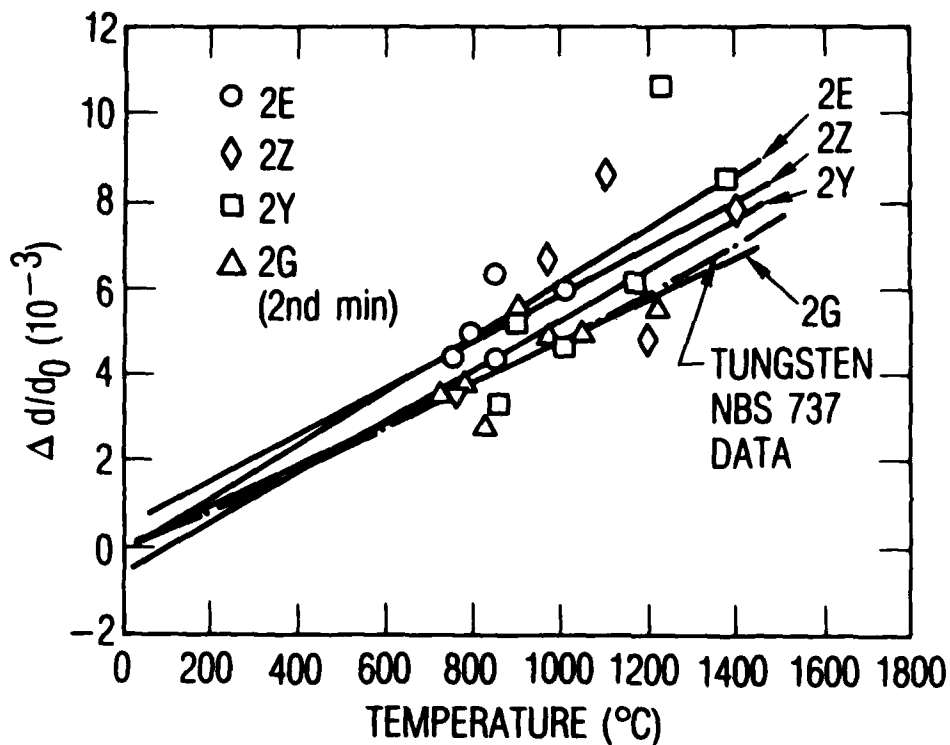


Figure 5. Thermal expansion $\Delta d/d_0$ versus temperature for tungsten filaments. Individual sample data are indicated. Lines were derived by linear regression through indicated data and a point (not shown) at room temperature defined as $\Delta d/d_0 = 0$. The broken line is from data on National Bureau of Standards NBS 737 tungsten standard reference material.

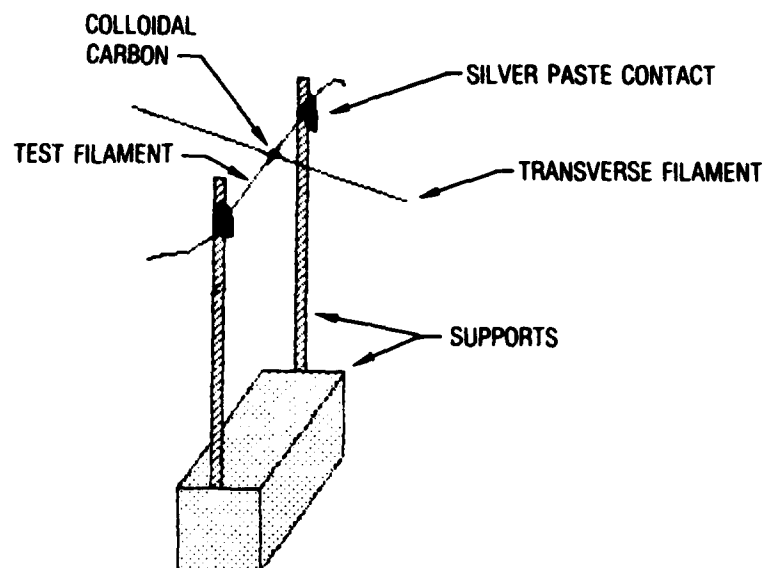


Figure 6. Apparatus for observing heating-induced twisting in carbon filaments. The transverse filament moves freely in response to twisting in the test filament. The fixture is enclosed in vacuum, and the ends of the transverse filament are observed in the direction of the test filament axis. The degree of twist is evaluated: $\theta = \sin^{-1}(s/l)$, where s = displacement of transverse filament end upon heating and l = length from test filament to transverse filament end.

explain this variation. The photomicrographs were taken under polarized light; the gross orientation of the graphitic layers in the filaments can be inferred from the filaments' optical textures. Note that the optical texture of the PAN filaments is symmetric with respect to the filament longitudinal axis, whereas that of the P55 filaments is not. With the PAN filaments, the structure traversed by any randomly drawn diametral chord does not vary as a function of polar angle of the chord. The same is not true for the P55 filaments, in which the graphitic layer planes tend to be aligned mostly parallel to the largest diameter of the filament cross section.^{6,7} Therefore, transverse thermal expansion measurements taken parallel to these layer planes should be different from those taken 90 deg to that direction because of the large difference in thermal expansivities of the two principal crystallographic directions in graphite. In other words, the P55 filaments would not be expected to expand equally in all radial directions. Since the filaments were mounted randomly in the expansion apparatus, different diameters having different characteristic thermal expansions were presented to the laser beam, resulting in an apparent CTE variation from filament to filament.

The transverse CTE values determined for the PAN filaments did not vary significantly either from filament to filament or as a function of filament type. The filament-to-filament uniformity is consistent with the polar symmetry present in the structure of these filaments when they are viewed in cross section (Fig. 1). Also, any twist that might have occurred during the test would have minimal effect on the data because the cross sections of these filaments have a low eccentricity. That the different types of PAN filaments did not vary significantly in transverse CTE is probably due to the fact that these fibers are essentially identical except for their manufacturing heat-treatment temperature. Since they were all heat-treated in-house to 2600°C prior to the experiment, there is no reason to expect the transverse CTE of these filaments to be significantly different.

The tungsten data plotted in Fig. 5 appear to have a larger data spread than the PAN filament data. The spread can be attributed to the plot's finer y-axis scale and the uncertainty in d_0 for the 2Y and 2Z specimens. As mentioned above, these specimens were undergoing irreversible diameter decreases

at elevated temperature, so $\Delta d/d_0$ was calculated for each room-temperature/elevated-temperature data pair, which causes a doubling of the noise level in the $\Delta d/d_0$ data for these runs.

Note that, for purposes of calculation, the transverse CTE of the filaments was assumed to be linear over the entire temperature range. This assumption appears reasonable for the more glassy PAN-type filaments but may be in error for the pitch-type filaments because of their more graphitic structure. Others have obtained similar values for the transverse CTE of PAN filaments at temperatures below those investigated here,^{8,9} indicating that the CTE of PAN filaments does not vary strongly as a function of temperature, and the assumption of linearity is adequate for them.

IV. CONCLUSIONS

The transverse CTE of high-temperature heat-treated carbon filaments is approximately linear from room temperature to 1600°C. The average value of the transverse CTE for the PAN filaments tested was $\sim 12 \times 10^{-6} \text{ }^{\circ}\text{C}^{-1}$; this value may differ for fibers that have not been heat-treated to high temperatures. The P55 filaments have a definite tendency to twist when they are heated. It is currently not known what effect such torque has on the micro-stress environment of a composite, or whether more-isotropic fibers display the same tendency.

Although the data are by no means exhaustive, there is strong evidence that the transverse CTE of the P55 filaments varies as a function of the particular diameter measured. This variation is theorized to be related to the microstructure of the filaments, i.e., the alignment of graphitic layer planes over lengths on the order of the filament diameter. The relationship between the transverse CTE anisotropy and the microstructures of the P55 and other anisotropic filaments must be characterized further. The few data taken indicate that the P55 transverse CTE values, averaged over all radial directions, are close to that of the PAN filaments (when they are heat-treated to similar temperatures). More work is necessary to investigate this closeness and to determine the effect of heat-treatment temperature on transverse CTE. The pyrolysis shrinkage behavior of carbon filaments, which is of importance particularly in carbon-carbon composite manufacture, can also be investigated by this technique.

REFERENCES

1. C. C. Chamis and G. P. Sendeckyj, J. Compos. Mater. 2, 332 (1968).
2. J. F. Helmer and R. J. Diefendorf, Ext. Abstr., 16th Biennial Conf. Carbon (1983), p. 511.
3. A. J. Perry, B. Ineichen, and B. Eliasson, J. Mater. Sci. 9, 1376 (1974).
4. W. Marciniak and F. Rozploch, High Temperatures - High Pressures, Vol. 11, (1979), pp. 709-710.
5. G. L. Kehl, The Principles of Metallographic Laboratory Practice, 3d ed., McGraw-Hill, New York (1949), pp. 490-494.
6. J. L. White, C. B. Ng, M. Buechler, and E. J. Watts, Ext. Abstr., 15th Biennial Conf. Carbon (1981), p. 310.
7. C. B. Ng, G. W. Henderson, M. Buechler, and J. L. White, Ext. Abstr., 16th Biennial Conf. Carbon (1983), p. 515.
8. J. J. Kiebler, K. W. Buesking, and J. Rabinsky, Exploratory Development of In-Process Yarn Bundle Properties, AFWAL-TR-80-4096 (July 1980).
9. R. C. Fanning and J. N. Fleck, Ext. Abstr., 10th Biennial Conf. Carbon (1971), p. 47.

LABORATORY OPERATIONS

The Aerospace Corporation functions as an "architect-engineer" for national security projects, specializing in advanced military space systems. Providing research support, the corporation's Laboratory Operations conducts experimental and theoretical investigations that focus on the application of scientific and technical advances to such systems. Vital to the success of these investigations is the technical staff's wide-ranging expertise and its ability to stay current with new developments. This expertise is enhanced by a research program aimed at dealing with the many problems associated with rapidly evolving space systems. Contributing their capabilities to the research effort are these individual laboratories:

Aerophysics Laboratory: Launch vehicle and reentry fluid mechanics, heat transfer and flight dynamics; chemical and electric propulsion, propellant chemistry, chemical dynamics, environmental chemistry, trace detection; spacecraft structural mechanics, contamination, thermal and structural control; high temperature thermomechanics, gas kinetics and radiation; cw and pulsed chemical and excimer laser development including chemical kinetics, spectroscopy, optical resonators, beam control, atmospheric propagation, laser effects and countermeasures.

Chemistry and Physics Laboratory: Atmospheric chemical reactions, atmospheric optics, light scattering, state-specific chemical reactions and radiative signatures of missile plumes, sensor out-of-field-of-view rejection, applied laser spectroscopy, laser chemistry, laser optoelectronics, solar cell physics, battery electrochemistry, space vacuum and radiation effects on materials, lubrication and surface phenomena, thermionic emission, photosensitive materials and detectors, atomic frequency standards, and environmental chemistry.

Computer Science Laboratory: Program verification, program translation, performance-sensitive system design, distributed architectures for spaceborne computers, fault-tolerant computer systems, artificial intelligence, microelectronics applications, communication protocols, and computer security.

Electronics Research Laboratory: Microelectronics, solid-state device physics, compound semiconductors, radiation hardening; electro-optics, quantum electronics, solid-state lasers, optical propagation and communications; microwave semiconductor devices, microwave/millimeter wave measurements, diagnostics and radiometry, microwave/millimeter wave thermionic devices; atomic time and frequency standards; antennas, rf systems, electromagnetic propagation phenomena, space communication systems.

Materials Sciences Laboratory: Development of new materials: metals, alloys, ceramics, polymers and their composites, and new forms of carbon; non-destructive evaluation, component failure analysis and reliability; fracture mechanics and stress corrosion; analysis and evaluation of materials at cryogenic and elevated temperatures as well as in space and enemy-induced environments.

Space Sciences Laboratory: Magnetospheric, auroral and cosmic ray physics, wave-particle interactions, magnetospheric plasma waves; atmospheric and ionospheric physics, density and composition of the upper atmosphere, remote sensing using atmospheric radiation; solar physics, infrared astronomy, infrared signature analysis; effects of solar activity, magnetic storms and nuclear explosions on the earth's atmosphere, ionosphere and magnetosphere; effects of electromagnetic and particulate radiations on space systems; space instrumentation.

